ACS APPLIED MATERIALS & INTERFACES

Research Article

www.acsami.org

Ultra-Low-Cost and Flexible Paper-Based Microplasma Generation Devices for Maskless Patterning of Poly(ethylene oxide)-like Films

Yao-Jhen Yang, Meng-Yu Tsai, Wei-Chieh Liang, Hsien-Yeh Chen,* and Cheng-Che Hsu*

Department of Chemical Engineering, National Taiwan University, Number 1, Section 4, Roosevelt Road, Taipei, Taiwan

ABSTRACT: This work presents the use of an ultra-low-cost and flexible paper-based microplasma array to perform maskless patterning of poly(ethylene oxide)-like (PEO-like) thin films with a feature size down to submillimeter scale. In this process, the liquid precursor was directly applied to the paper substrate, gradually vaporized, and dissociated in the microplasma cavity, which leads to plasma polymerization. The FTIR and XPS spectra of the deposited film confirm the PEO-like structures. The protein adsorption test using the absorption of fluorescence-labeled fibrinogen conjugates on the treated surface shows the deposited films possessed the antifouling property with decent pattern transfer fidelity defined by the geometry of the microplasma array.

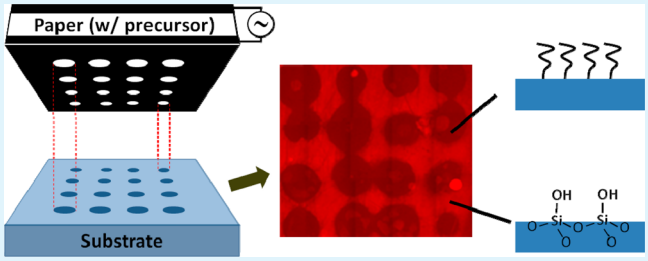

KEYWORDS: *microplasma, paper-based device, polymerization, poly(ethylene oxide), maskless patterning*

1. INTRODUCTION

Atmospheric pressure (AP) microplasmas are plasmas ignited at 1 atm with at least one geometric dimension equal to or less than 1 mm. Due to the confined discharge volume, such a type of plasmas offers a highly reactive environment in a confined area. Additionally, with the feature of no need for expensive vacuum facilities, AP microplasma offers a lot of possibilities and has been widely utilized in various applications such as photonic devices,[1,2] surface modification,[3−5] material deposition,[6,7] and biomedical applications.[8−10] Several of the above applications involve maskless patterning on surfaces.[11−16] Among AP microplasmas, various systems have been developed, as summarized in review papers.[17−21] Due to their small size, they are especially suitable for applications where localized reaction or treatment is desired.

Extensive effort has been made in the development of paper-based devices due to the fact that paper substrates are cheap and flexible and can be obtained easily. Various types of paper-based devices have been reported, such as biochips,[22,23] microfluidic devices,[24,25] and electronic devices.[26−29] The development of paper-based plasma-generation devices has created new venues toward various plasma-assisted processes.[30,31] Such plasma-generation devices serve as a cost-effective and flexible platform for several applications such as plasma spectroscopy and localized surface treatment. The microstructure of paper allows for liquid storage and/or transportation on the substrate. By integration of such a feature and the highly localized environment of the microplasmas, such a paper-based plasma generation device can be used to perform localized thin-film deposition.

Poly(ethylene oxide) (PEO) is known as a protein-repelling material.[32,33] Such a material can protect surfaces in contact with physiological fluids from the adsorption of biomolecules. PEO films can be deposited using various processes, such as chemical grafting,[34,35] self-assembly,[36,37] pulsed laser deposition,[38] initiated chemical vapor deposition,[39] and plasma-assisted processes. Among these processes, various plasma-assisted processes utilizing plasma polymerization with low pressure[40−43] and AP plasmas have been reported. Nisol et al.[44] and Gordeev et al.[45] reported a process by directly injecting the precursor into the plasma system. Such a precursor injection scheme has been widely employed and may require heating elements to ensure that a sufficient amount of the precursor vapor is injected. When surface patterning is desired, an extra lithographic step is typically required.

In this work, we present a paper-based microplasma-generation device that creates a discharge array for maskless patterning of PEO-like films with a spatial resolution down to submillimeter scale without the need for extra bubbling or heating systems. The precursor, tetraglyme, was adsorbed in the paper substrate, gradually vaporized, and reacted with the microplasma for plasma polymerization occurring in designated locations. The microplasma was diagnosed optically and electrically. PEO-like films were characterized by FTIR and XPS. The antifouling behavior was examined with the absorption of Alexa Fluor 546-conjugated fibrinogen on the designated locations.

2. EXPERIMENTAL PROCEDURE

The paper-based microdischarge array device has been demonstrated and described previously.[31] In brief, it consists of paper-based ground and powered electrodes and a dielectric barrier between the two electrodes. The ground electrode was made of paper coated with

Received: April 23, 2014
Accepted: July 15, 2014
Published: July 15, 2014

conductive carbon pastes. Scotch tape was used as the dielectric layer. The powered electrode consisted of a layer of double-sided tape attached to the backside of the carbon-coated paper. Discharge cavities were defined by perforations through the power electrode using a 25 G puncher with an outer diameter of 500 μm. A device with a 4 × 4 array was used in this work. The device is flexible itself, and the variation in power consumption of the device is well below 10% after 100 bending cycles on a surface with a radius of curvature of 4.5 mm. The lifetime of this device is at least 55 min when being operated under an Ar atmosphere with proper operating conditions. For maskless patterning of PEO-like thin films, 15 μL of the precursor liquid (tetraglyme, $CH_3O(CH_2CH_2O)_4CH_3$, Aldrich, 99%) was absorbed in the paper of the power electrode. Figure 1a shows a schematic of the device cross

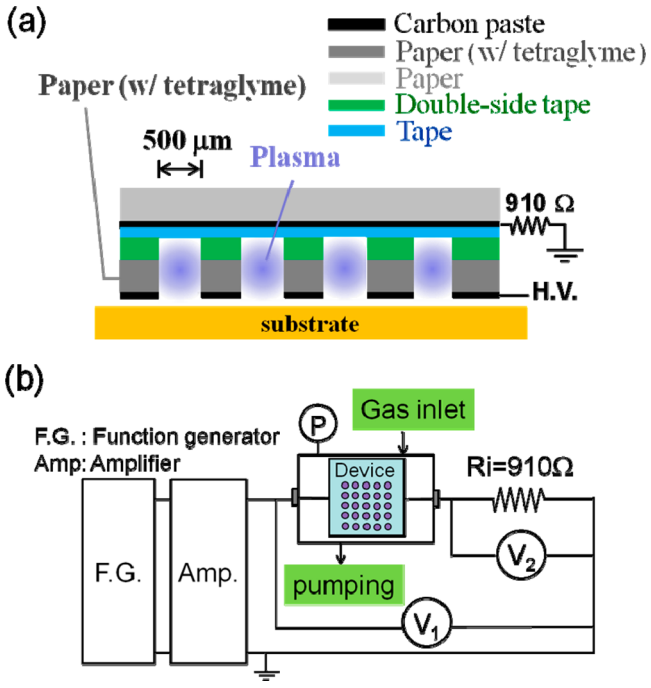

Figure 1. Schematic of the paper-based microarray system for PEO-like thin film deposition: (a) cross-section view of the device and (b) circuitry of the system. The schematic is not to scale.

section. During the PEO-like materials patterning process, a substrate was firmly attached to the device. When the plasma was ignited, the liquid precursor was partially vaporized, diffused into the cavities, and reacted with plasmas. By using this device, no additional heating source is needed to vaporize the precursor into the cavities, and the precursor can be distributed to each cavity evenly.

Figure 1b shows a schematic of the experimental setup. A 50 kHz sinusoidal wave with a duty cycle of 10% and a repetition frequency of 1 kHz generated by a function generator (ww1071, Tabor Electronics Ltd.) was amplified by an amplifier (5/80, Trek) and applied to the device. The device was placed in an ambient-controlled chamber and was connected in series with a 910 Ω resistor (Ri) to measure the current on the basis of Ohm's law. To minimize the ambient gas contamination in the patterning step, the chamber was pumped down and then filled up with the plasma gas at a flow rate of 570 sccm before each coating process. The voltages across the system and across Ri were monitored by voltage probes V_1 (P5100A, Tektronix) and V_2 (P2221, Tektronix), respectively. The discharge voltage reported in this work is the root-mean-square voltage across the device unless otherwise specified. The plasma emission spectra were obtained by the optical emission spectrometer (SP2500i, Princeton Instrument).

The deposited patterned films were analyzed by FTIR (Spectrum 100, PerkinElmer) and XPS (VG ESCA Scientific Theta Probe). Au-coated silicon wafers were used as a substrate for samples for FTIR and XPS analyses. An FTIR spectrometer equipped with an attenuated total reflectance (ATR) module was used, and the resolution of the spectra was 4 cm^{-1}. A ZnSe crystal was used in the ATR module, and the depth of penetration was about 2 μm at 1000 cm^{-1}. In XPS analyses, the samples deposited with PEO-like films were irradiated by a monochromatic Al Kα X-ray source (1486.6 eV) with a spot size of 400 μm and a takeoff angle of 53°. For each measurement, the samples were cleaned by an Ar ion gun for 2 s first to remove the potential contamination.

The fouling property of the deposited PEO-like patterns was studied using protein adsorption tests. In this test, PEO-like films were deposited on glass substrates (plane, FEA). Alexa Fluor 546-conjugated fibrinogen was utilized as a model reporter molecule, and the protein solutions were prepared at a concentration of 100 μg/mL. The patterned substrates were incubated in the protein solution for 10 min and then washed three times with phosphate-buffered saline (PBS) (Sigma, pH 7.4, contains 0.05% Tween 20) and once more with PBS (Sigma, pH 7.4) to rinse off the excess adsorbed proteins. The prepared samples were examined by a fluorescence microscope (NikonTE2000-U).

3. EXPERIMENTAL RESULTS

The behavior of plasmas generated by the paper-based device with and without the introduction of a liquid precursor was first investigated. To simulate the plasma behavior during the PEO-like thin film deposition process, the power electrode was firmly attached to a glass substrate and a voltage of 700 V was applied to the device. Parts a and b of Figure 2 show the voltage and current waveforms of the plasmas ignited without and with the introduction of the precursor, respectively. The current waveforms show several current spikes superimposed onto the sinusoidal displacement current. To more clearly show the difference in the current waveforms, the detailed structures are shown in the inset of these two figures. Such current waveforms clearly indicate that the discharge is filamentary in nature.[46,47] They clearly show that, with the introduction of a precursor liquid, the number and amplitude of current spikes decrease, suggesting quenching of the discharge with the addition of the precursor vapor. The power consumptions under these two conditions were less than 0.1 W on the basis of Lissajous plots.[48,49]

The visual appearances of the devices with and without the addition of the precursor are also shown (Figure 2c). Plasmas were ignited in all 16 cavities of the 4 × 4 array. A weaker visible light emission intensity was observed for the device ignited at ambient with the addition of the precursor. Such an observation is consistent with the current waveform measurements shown above. The optical emission spectra emanating from the plasma were also examined and are shown in Figure 2d. We observed much stronger emission line intensities for the case without precursor addition. When the precursor is vaporized and reacted with plasma, the excited-state species is quenched by inelastic collisions with species generated by the precursor molecules. In addition, a certain amount of energy is consumed on dissociation of the precursor molecules, resulting in a decrease in the current spike amplitude and the light intensity.[50]

Figure 3 shows the visual appearances of the device ignited with voltages of 500, 600, and 700 V. We first note that no plasma emission was observed with an applied voltage below 400 V. With an increase in the applied voltage, ignition of the plasmas in the cavities occurred. With an applied voltage not sufficiently high, e.g., 500 and 600 V, plasmas were only ignited in part of the cavities. This cavity-to-cavity emission intensity variation is likely due to the nonuniform nature of the paste and paper substrate, as well as the fabrication process. At an optimal

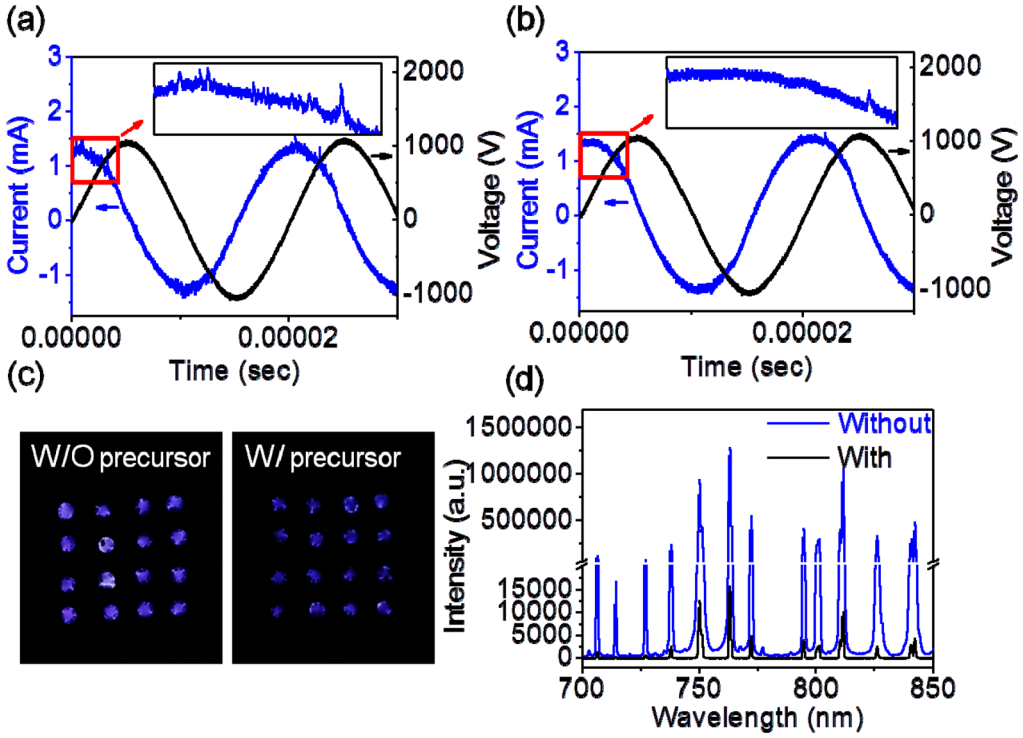

Figure 2. Current and voltage waveforms of the plasmas ignited (a) without and (b) with the introduction of the precursor. (c) Visual appearances and (d) optical emission spectra under with- and without-precursor conditions. The plasmas were ignited at 700 V.

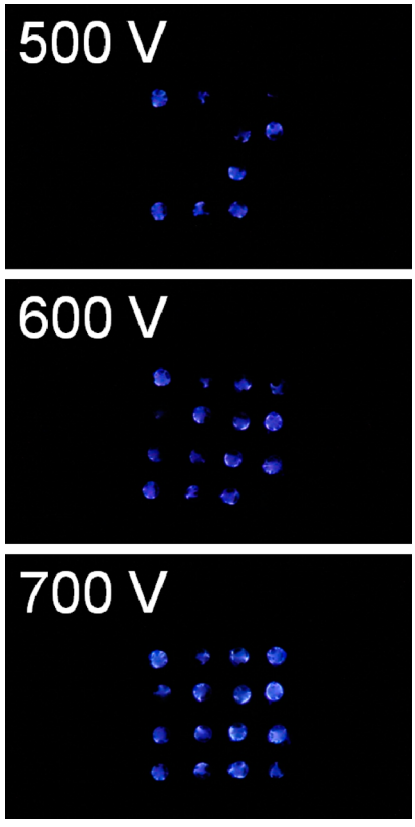

Figure 3. Visual appearances of the devices at different applied voltages.

applied voltage of 700 V, the plasmas were stably ignited in each cavity. A further increase in the applied voltage will lead to undesirable breakdown and eventually damage of the device. An increase in the frequency of the applied voltage plays the same role as an increase in the applied voltage and is therefore not further discussed.

Parts a and b of Figure 4 show the FTIR spectra of the precursor and patterns deposited under different applied voltages, respectively. The tetraglyme spectrum shows the absorptions of the O−H stretching vibration (3200−3500 cm^{-1}), C−H stretching vibration (2800−3000 cm^{-1}), C−H scissoring vibration (~1450 cm^{-1}), and C−O−C stretching vibration (~1100 cm^{-1}), which are consistent with those reported in the literature.[44] The patterns of the films deposited at voltages ranging from 500 to 700 V after 10 min of deposition were examined by FTIR analyses. This analysis was performed at a selective area where plasma polymerization occurs. The results show stronger absorption peaks with an applied voltage of 700 V. The peak intensities decrease with the applied voltage. Under 500 V of applied voltage, rather weak absorption peaks were observed. At a lower operating voltage, the lower plasma density leads to a lower deposition rate, which leads to the formation of a much thinner film thickness. By comparing the spectra of the sample deposited at 700 V and tetraglyme, we found good retention of the C−O−C stretching vibration at 1100 cm^{-1}, suggesting the functionality is retained and the antifouling property is therefore expected.[51,52] An additional C═O peak at 1730 cm^{-1} was observed, and it was attributed to the destruction and rearrangement of the backbone of the precursor.

The elemental composition and chemical environments of deposited PEO-like thin films were further examined by XPS. The patterned thin films to be characterized were deposited on a Au-coated Si wafer for 150 s. To demonstrate that the patterns were deposited only on designated regions, namely, the location where discharges occurred, XPS survey scan spectra of the sample on deposition and nondeposition regions

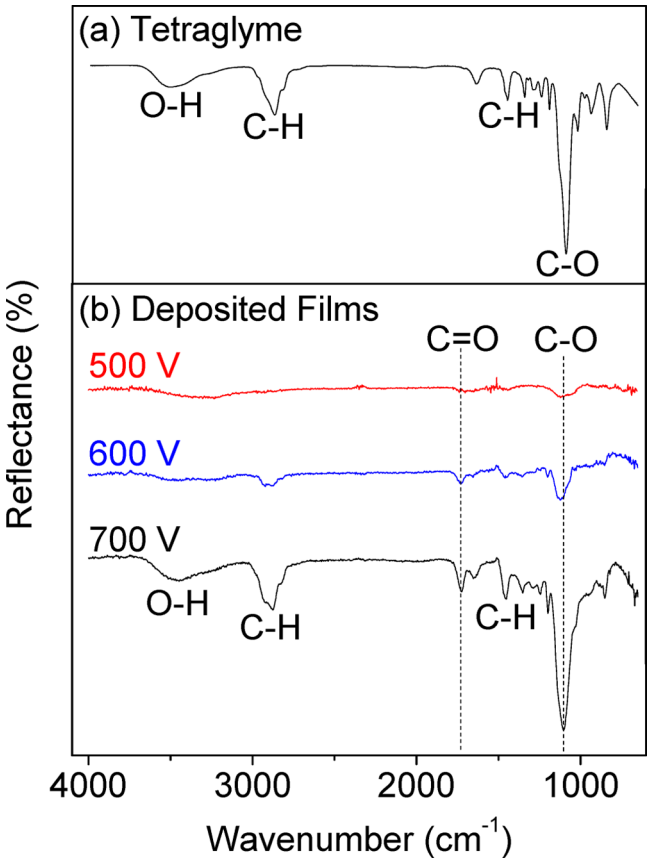

Figure 4. FTIR spectra of (a) tetraglyme and (b) the deposited films at different applied voltages.

were acquired. Figure 5 shows the survey scan of the deposition and nondeposition regions. On the deposition region, the

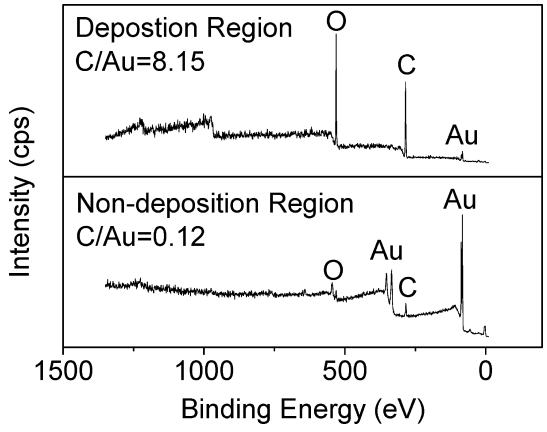

Figure 5. XPS survey scan spectra of (a, top) deposition and (b, bottom) nondeposition regions of the sample prepared at 700 V.

carbon and oxygen peaks dominate the spectrum, and the intensity ratio of carbon to gold is 8.15, while the C/Au ratio is 0.12 on the nondeposition region. This clearly shows that plasma polymerization occurs in the designated areas. The probing depth of the XPS analysis is several nanometers near the surface with an X-ray spot size of 400 μm. The Au signal on the deposition region can come from the vicinity of the nondeposition region due to slight misalignment of the patterned area. The results suggest the capability of surface patterning of the device without the need for additional masks.

Figure 6 shows the detailed carbon scan of the samples deposited under various applied voltages. The C peaks were

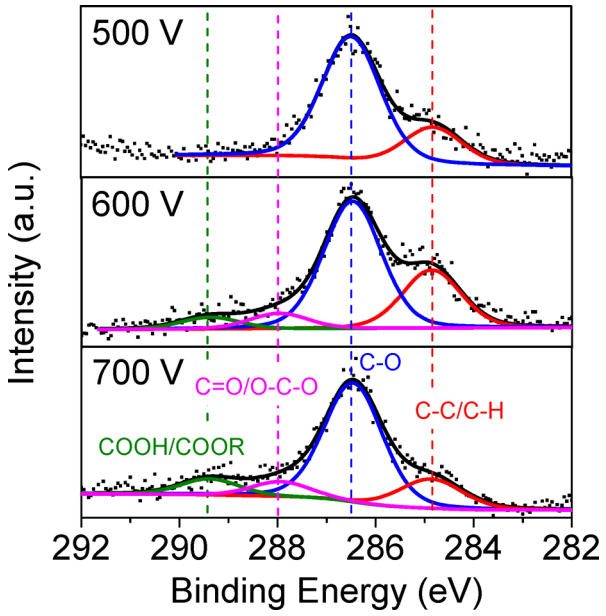

Figure 6. XPS C 1s high-resolution scan spectra of the deposited films prepared under different applied voltages.

deconvoluted into four components at 284.8 eV (C−C/C−H groups), 286.5 eV (C−O groups), 288 eV (C═O/O−C−O groups), and 289.5 eV (COOH/COOR groups).[44] The C−O peak at 286.5 eV is the typical bonding of PEO, and the relative abundance indicates the retention of the functionality after the polymerization process. The presence of C═O/O−C−O groups and COOH/COOR groups is attributed to the dissociation of the precursor molecules by the plasmas, indicating a certain degree of destruction of precursor molecules. This figure shows that, with an increase in the applied voltage, the percentages of C═O/O−C−O and COOH/COOR bonding increase. This effect can be explained by a higher plasma density at higher applied voltage, increasing the degree of dissociation of the precursor molecules, as reported in the literature.[40,44,52]

The antifouling property of the deposited films was examined by using Alexa Fluor 546-conjugated fibrinogen as model molecules. On the regions deposited with PEO-like thin films, the thin film hindered the adsorption of fibrinogen molecules, resulting in the dark regions in the image, while the rest of the regions were covered by fluorescently labeled fibrinogen conjugates and displayed red color in the fluorescence microscope. Figure 7 shows the visual appearances of the device when the plasma is ignited and corresponding fluorescence images of the sample processed at 600 and 700 V after the maskless patterning of PEO-like films. Since obtaining the mirror-reflected patterns is the feature of this patterning method, the mirrored images of the fluorescence microscope images are presented. Under the optimal conditions (700 V), they show clear contrast between 4 × 4 black array and red areas. Under 600 V, only a portion of the 4 × 4 spots exhibit the antifouling property since plasmas were not ignited in every cavity under this applied voltage. The size

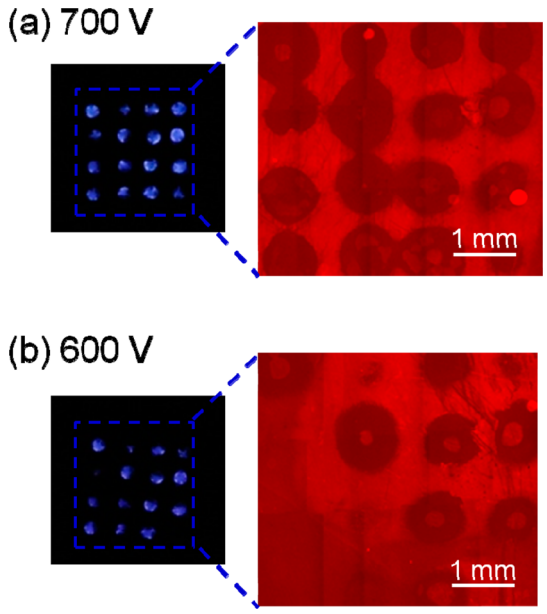

Figure 7. Fluorescence image of the sample processed at (a) 700 V and (b) 600 V after the protein incubation procedures.

of the antifouling spots is somewhat larger than that of the discharge region. This is due to the lateral diffusion of the species during the process. We note that the shape and size of the antifouling spots are not as clearly defined as those shown in the literature.[53] This is a result of the nonuniform nature of this ultra-low-cost plasma-generation device.

4. CONCLUSION

An ultra-low-cost and flexible paper-based array microplasma-generation device was used to perform the patterning of PEO-like thin films. This is a maskless surface patterning process. In this process, a precursor liquid was absorbed in the paper substrates and vaporized to react with plasmas during the polymerization process. The FTIR and XPS spectra of the deposited films show good retention of ether structures during the polymerization process. To examine the antifouling property, the protein adsorption test was performed. The fluorescence image shows contrast between the regions with and without deposition, and the pattern follows the geometry on the electrode. Submillimeter feature sizes can be obtained using this process.

We note that several state-of-the-art techniques such as lithographic, laser-assisted, and nanoimprinting processes are able to perform surface patterning with better patterning spatial resolution. These techniques, however, require sophisticated equipment and/or complicated operating procedures. The intention of this work was to present a facile and cost-effective method for patterning submillimeter features. This technique is able to perform maskless patterning with an ultra-low-cost device (composed of paper, tape, and carbon paste) within one step. The desired patterns can be transferred to the substrates in a very simple manner. Furthermore, by utilizing the capillary phenomena of paper fibers, this process is capable of handling a liquid precursor without the need for additional heater or bubbler systems. This process is flexible in two senses: first, the paper-based device itself is flexible; second, this device can be fabricated into arbitrary shapes to fit the need of various applications. Such ultra-low-cost and flexible features allow the utilization of such a device in various applications.

AUTHOR INFORMATION

Corresponding Authors

*E-mail: hsychen@ntu.edu.tw.
*E-mail: chsu@ntu.edu.tw.

Notes

The authors declare no competing financial interest.

ACKNOWLEDGMENTS

This work was supported by the National Science Council of Taiwan, ROC (Grant NSC 101-2221-E-002-163-MY2).

REFERENCES

(1) Eden, J. G.; Park, S. J. Microcavity Plasma Devices and Arrays: A New Realm of Plasma Physics and Photonic Applications. *Plasma Phys. Controlled Fusion* **2005**, *47*, B83−B92.
(2) Park, S. J.; Chen, K. F.; Ostrom, N. P.; Eden, J. G. 40,000 Pixel Arrays of AC-Excited Silicon Microcavity Plasma Devices. *Appl. Phys. Lett.* **2005**, *86*, 111501.
(3) Lucas, N.; Ermel, V.; Kurrat, M.; Buettgenbach, S. Microplasma Stamps for Selective Surface Modification: Design and Characterization. *J. Phys. D: Appl. Phys.* **2008**, *41*, 215202.
(4) West, J.; Michels, A.; Kittel, S.; Jacob, P.; Franzke, J. Microplasma Writing for Surface-Directed Millifluidics. *Lab Chip* **2007**, *7*, 981−983.
(5) Szili, E. J.; Al-Bataineh, S. A.; Ruschitzka, P.; Desmet, G.; Priest, C.; Griesser, H. J.; Voelcker, N. H.; Harding, F. J.; Steele, D. A.; Short, R. D. Microplasma Arrays: A New Approach for Maskless and Localized Patterning of Materials Surfaces. *RSC Adv.* **2012**, *2*, 12007−12010.
(6) Al-Bataineh, S. A.; Szili, E. J.; Gruner, P. J.; Priest, C.; Griesser, H. J.; Voelcker, N. H.; Short, R. D.; Steele, D. A. Fabrication and Operation of a Microcavity Plasma Array Device for Microscale Surface Modification. *Plasma Processes Polym.* **2012**, *9*, 638−646.
(7) Nozaki, T.; Sasaki, K.; Ogino, T.; Asahi, D.; Okazaki, K. Microplasma Synthesis of Tunable Photoluminescent Silicon Nanocrystals. *Nanotechnology* **2007**, *18*, 235603.
(8) Kim, S. J.; Chung, T. H.; Bae, S. H.; Leem, S. H. Bacterial Inactivation Using Atmospheric Pressure Single Pin Electrode Microplasma Jet with a Ground Ring. *Appl. Phys. Lett.* **2009**, *94*, 141502.
(9) Uhm, H. S.; Hong, Y. C. Various Microplasma Jets and Their Sterilization of Microbes. *Thin Solid Films* **2011**, *519*, 6974−6980.
(10) North, S. H.; Lock, E. H.; Cooper, C. J.; Franek, J. B.; Taitt, C. R.; Walton, S. G. Plasma-Based Surface Modification of Polystyrene Microtiter Plates for Covalent Immobilization of Biomolecules. *ACS Appl. Mater. Interfaces* **2010**, *2*, 2884−2891.
(11) Al-Bataineh, S. A.; Short, R. D. Protein Patterning on Microplasma-Activated PEO-like Coatings. *Plasma Processes Polym.* **2014**, *11*, 263−268.
(12) Weng, C. C.; Hsueh, J. C.; Liao, J. D.; Chen, C. H.; Yoshimura, M. Rapid Micro-Scale Patterning of Alkanethiolate Self-Assembled Monolayers on Au Surface by Atmospheric Micro-Plasma Stamp. *Plasma Processes Polym.* **2013**, *10*, 345−352.
(13) Ghosh, S.; Yang, R.; Kaumeyer, M.; Zorman, C. A.; Rowan, S. J.; Feng, P. X. L.; Sankaran, R. M. Fabrication of Electrically Conductive Metal Patterns at the Surface of Polymer Films by Microplasma-Based Direct Writing. *ACS Appl. Mater. Interfaces* **2014**, *6*, 3099−3104.
(14) Huiskamp, T.; Brok, W. J. M.; Stevens, A. A. E.; van Heesch, E. J. M.; Pemen, A. J. M. Maskless Patterning by Pulsed-Power Plasma Printing. *IEEE Trans. Plasma Sci.* **2012**, *40*, 1913−1925.
(15) Ideno, T.; Ichiki, T. Maskless Etching of Microstructures Using a Scanning Microplasma Etcher. *Thin Solid Films* **2006**, *506−507*, 235−238.
(16) Sankaran, R. M.; Giapis, K. P. Maskless Etching of Silicon Using Patterned Microdischarges. *Appl. Phys. Lett.* **2001**, *79*, 593−595.

(17) Foest, R.; Schmidt, M.; Becker, K. Microplasmas, an Emerging Field of Low-Temperature Plasma Science and Technology. *Int. J. Mass Spectrom.* **2006**, *248*, 87−102.
(18) Iza, F.; Kim, G. J.; Lee, S. M.; Lee, J. K.; Walsh, J. L.; Zhang, Y. T.; Kong, M. G. Microplasmas: Sources, Particle Kinetics, and Biomedical Applications. *Plasma Processes Polym.* **2008**, *5*, 322−344.
(19) Tachibana, K. Current Status of Microplasma Research. *IEEJ Trans. Electr. Electron. Eng.* **2006**, *1*, 145−155.
(20) Karanassios, V. Microplasmas for Chemical Analysis: Analytical Tools or Research Toys? *Spectrochim. Acta, Part B* **2004**, *59*, 909−928.
(21) Davide, M.; Sankaran, R. M. Microplasmas for Nanomaterials Synthesis. *J. Phys. D: Appl. Phys.* **2010**, *43*, 323001.
(22) Dungchai, W.; Chailapakul, O.; Henry, C. S. Electrochemical Detection for Paper-Based Microfluidics. *Anal. Chem.* **2009**, *81*, 5821−5826.
(23) Cheng, C. M.; Martinez, A. W.; Gong, J.; Mace, C. R.; Phillips, S. T.; Carrilho, E.; Mirica, K. A.; Whitesides, G. M. Paper-Based ELISA. *Angew. Chem., Int. Ed.* **2010**, *49*, 4771−4774.
(24) Martinez, A. W.; Phillips, S. T.; Nie, Z. H.; Cheng, C. M.; Carrilho, E.; Wiley, B. J.; Whitesides, G. M. Programmable Diagnostic Devices Made from Paper and Tape. *Lab Chip* **2010**, *10*, 2499−2504.
(25) Carrilho, E.; Martinez, A. W.; Whitesides, G. M. Understanding Wax Printing: A Simple Micropatterning Process for Paper-Based Microfluidics. *Anal. Chem.* **2009**, *81*, 7091−7095.
(26) Manekkathodi, A.; Lu, M. Y.; Wang, C. W.; Chen, L. J. Direct Growth of Aligned Zinc Oxide Nanorods on Paper Substrates for Low-Cost Flexible Electronics. *Adv. Mater.* **2010**, *22*, 4059−4063.
(27) Siegel, A. C.; Phillips, S. T.; Dickey, M. D.; Lu, N. S.; Suo, Z. G.; Whitesides, G. M. Foldable Printed Circuit Boards on Paper Substrates. *Adv. Funct. Mater.* **2010**, *20*, 28−35.
(28) Mazzeo, A. D.; Kalb, W. B.; Chan, L.; Killian, M. G.; Bloch, J. F.; Mazzeo, B. A.; Whitesides, G. M. Paper-Based, Capacitive Touch Pads. *Adv. Mater.* **2012**, *24*, 2850−2856.
(29) Kim, D. Y.; Steckl, A. J. Electrowetting on Paper for Electronic Paper Display. *ACS Appl. Mater. Interfaces* **2010**, *2*, 3318−3323.
(30) Hsu, C. C.; Tsai, J. H.; Yang, Y. J.; Liao, Y. C.; Lu, Y. W. A Foldable Microplasma-Generation Device on a Paper Substrate. *J. Microelectromech. Syst.* **2012**, *21*, 1013−1015.
(31) Yang, Y. J.; Hsu, C. C. A Flexible Paper-Based Microdischarge Array Device for Maskless Patterning on Nonflat Surfaces. *J. Microelectromech. Syst.* **2013**, *22*, 256−258.
(32) Jeon, S. I.; Lee, J. H.; Andrade, J. D.; De Gennes, P. G. Protein-Surface Interactions in the Presence of Polyethylene Oxide: I. Simplified Theory. *J. Colloid Interface Sci.* **1991**, *142*, 149−158.
(33) Castner, D. G.; Ratner, B. D. Biomedical Surface Science: Foundations to Frontiers. *Surf. Sci.* **2002**, *500*, 28−60.
(34) Sileika, T. S.; Kim, H. D.; Maniak, P.; Messersmith, P. B. Antibacterial Performance of Polydopamine-Modified Polymer Surfaces Containing Passive and Active Components. *ACS Appl. Mater. Interfaces* **2011**, *3*, 4602−4610.
(35) Delamarche, E.; Geissler, M.; Bernard, A.; Wolf, H.; Michel, B.; Hilborn, J.; Donzel, C. Hydrophilic Poly(dimethylsloxane) Stamps for Microcontact Printing. *Adv. Mater.* **2001**, *13*, 1164−1167.
(36) Rundqvist, J.; Hoh, J. H.; Haviland, D. B. Substrate Effects in Poly(ethylene glycol) Self-Assembled Monolayers on Granular and Flame-Annealed Gold. *J. Colloid Interface Sci.* **2006**, *301*, 337−341.
(37) Kim, P.; Lee, S. E.; Jung, H. S.; Lee, H. Y.; Kawai, T.; Suh, K. Y. Soft Lithographic Patterning of Supported Lipid Bilayers onto a Surface and Inside Microfluidic Channels. *Lab Chip* **2006**, *6*, 54−59.
(38) Bubb, D. M.; Ringeisen, B. R.; Callahan, J. H.; Galicia, M.; Vertes, A.; Horwitz, J. S.; McGill, R. A.; Houser, E. J.; Wu, P. K.; Pique, A.; Chrisey, D. B. Vapor Deposition of Intact Polyethylene Glycol Thin Films. *Appl. Phys. A: Mater. Sci. Process.* **2001**, *73*, 121−123.
(39) Bose, R. K.; Nejati, S.; Stufflet, D. R.; Lau, K. K. S. Graft Polymerization of Anti-Fouling PEO Surfaces by Liquid-Free Initiated Chemical Vapor Deposition. *Macromolecules* **2012**, *45*, 6915−6922.
(40) Palumbo, F.; Favia, P.; Vulpio, M.; d'Agostino, R. RF Plasma Deposition of PEO-Like Films: Diagnostics and Process Control. *Plasmas Polym.* **2001**, *6*, 163−174.
(41) Brétagnol, F.; Ceriotti, L.; Lejeune, M.; Papadopoulou-Bouraoui, A.; Hasiwa, M.; Gilliland, D.; Ceccone, G.; Colpo, P.; Rossi, F. Functional Micropatterned Surfaces by Combination of Plasma Polymerization and Lift-Off Processes. *Plasma Processes Polym.* **2006**, *3*, 30−38.
(42) Sardella, E.; Gristina, R.; Senesi, G. S.; d'Agostino, R.; Favia, P. Homogeneous and Micro-Patterned Plasma-Deposited PEO-like Coatings for Biomedical Surfaces. *Plasma Processes Polym.* **2004**, *1*, 63−72.
(43) Michelmore, A.; Gross-Kosche, P.; Al-Bataineh, S. A.; Whittle, J. D.; Short, R. D. On the Effect of Monomer Chemistry on Growth Mechanisms of Nonfouling PEG-like Plasma Polymers. *Langmuir* **2013**, *29*, 2595−2601.
(44) Nisol, B.; Poleunis, C.; Bertrand, P.; Reniers, F. Poly(ethylene glycol) Films Deposited by Atmospheric Pressure Plasma Liquid Deposition and Atmospheric Pressure Plasma-Enhanced Chemical Vapour Deposition: Process, Chemical Composition Analysis and Biocompatibility. *Plasma Processes Polym.* **2010**, *7*, 715−725.
(45) Gordeev, I.; Choukourov, A.; Simek, M.; Prukner, V.; Biederman, H. PEO-like Plasma Polymers Prepared by Atmospheric Pressure Surface Dielectric Barrier Discharge. *Plasma Processes Polym.* **2012**, *9*, 782−791.
(46) Kogelschatz, U. Filamentary, Patterned, and Diffuse Barrier Discharges. *IEEE Trans. Plasma Sci.* **2002**, *30*, 1400−1408.
(47) Wagner, H. E.; Brandenburg, R.; Kozlov, K. V.; Sonnenfeld, A.; Michel, P.; Behnke, J. F. The Barrier Discharge: Basic Properties and Applications to Surface Treatment. *Vacuum* **2003**, *71*, 417−436.
(48) Okazaki, S.; Kogoma, M.; Uehara, M.; Kimura, Y. Appearance of Stable Glow Discharge in Air, Argon, Oxygen and Nitrogen at Atmospheric-Pressure Using a 50-Hz Source. *J. Phys. D: Appl. Phys.* **1993**, *26*, 889−892.
(49) Zoran, F.; John, J. C. Microdischarge Behaviour in the Silent Discharge of Nitrogen - Oxygen and Water - Air Mixtures. *J. Phys. D: Appl. Phys.* **1997**, *30*, 817−825.
(50) Hsu, C. C.; Nierode, M. A.; Coburn, J. W.; Graves, D. B. Comparison of Model and Experiment for Ar, Ar/O 2 and Ar/O 2 /Cl_2 Inductively Coupled Plasmas. *J. Phys. D: Appl. Phys.* **2006**, *39*, 3272.
(51) Löpez, G. P.; Ratner, B. D.; Tidwell, C. D.; Haycox, C. L.; Rapoza, R. J.; Horbett, T. A. Glow Discharge Plasma Deposition of Tetraethylene Glycol Dimethyl Ether for Fouling-Resistant Biomaterial Surfaces. *J. Biomed. Mater. Res.* **1992**, *26*, 415−439.
(52) Wu, Y. J.; Timmons, R. B.; Jen, J. S.; Molock, F. E. Non-Fouling Surfaces Produced by Gas Phase Pulsed Plasma Polymerization of an Ultra Low Molecular Weight Ethylene Oxide Containing Monomer. *Colloids Surf., B* **2000**, *18*, 235−248.
(53) Tsai, M. Y.; Lin, C. Y.; Huang, C. H.; Gu, J. A.; Huang, S. T.; Yu, J.; Chen, H. Y. Vapor-Based Synthesis of Maleimide-Functionalized Coating for Biointerface Engineering. *Chem. Commun.* **2012**, *48*, 10969−10971.